Solvation and ionisation of alkali metals in liquid ammonia: a path integral Monte Carlo study

1990 J. Phys.: Condens. Matter 2 5833

(http://iopscience.iop.org/0953-8984/2/26/021)

J. Phys.: Condens. Matter 2 (1990) 5833–5848. Printed in the UK

Solvation and ionisation of alkali metals in liquid ammonia: a path integral Monte Carlo study

Massimo Marchi†§, Michiel Sprik‖ and Michael L Klein‡

† Department of Chemistry, McMaster University, Hamilton, Ontario, L8S 4M1, Canada

‡ Department of Chemistry and Laboratory for Reserch into the Structure of Matter, University of Pennsylvania, Philadelphia, PA 19104-6323, USA

Received 15 April 1990

Abstract. Quantum path integral Monte Carlo calculations have been used to study the properties of the alkali atoms Li, Na and Cs immersed in liquid ammonia. The solvent has been treated using a pairwise additive intermolecular potential fitted to experimental data. The alkali-atom solvent potential consists of two parts: an ion-core–solvent interaction fitted to quantum chemical calculations and a valence-electron–solvent pseudopotential taken from the solid-state literature. Two distinct forms of pseudopotential have been employed, one having an attractive, and the other a repulsive core. In the latter case, the equilibrium structure of Na and Cs is found to be an ionised state consisting of a fully solvated ion core, plus a well-separated, compact, solvated valence electron. In the case of Li, the equilibrium structure for both models appears to be a dipolar or excitonic atom. The relative merits of the two models are discussed and, where possible, contact is made with data on metal–ammonia solutions.

1. Introduction

Alkali metal–ammonia solutions have been the subject of intensive investigations [1–3]. The focus of most of these studies has been the transition from non-metallic to metallic properties which metal–ammonia solutions undergo at very low concentration of the alkali. The transition is signalled by a dramatic change in colour, from dark blue to metallic bronze, and a simultaneous rise in the conductivity of the solution. Remarkably, most transport properties of metal–ammonia solutions show small dependence on the type of alkali ion present.

Mean-field approaches have been used to rationalise the electronic conductivity in the high concentration regime [4, 5]. These theories consider the conduction electrons as nearly free, moving in an average potential field created by the solvated positive ions and the dipole moments of the solvent ammonia molecules; local fluctuations in the potential field are neglected. Clearly, continuum theories cannot be utilised in studying phenomena where the microscopic structure of the solvent plays a significant role, as in the process of atomic ionisation in solution. In this case, different theoretical techniques

§ Present address: Department of Chemistry, UC Berkeley, Berkeley, CA 94720, USA.

‖ Present address: IBM Zurich Research Laboratory, Rüschlikon, 8803 Switzerland.

0953-8984/90/265833 + 16 $03.50

must be employed, which, from the outset, allow a more realistic description of the solvent.

In a previous paper [6], we have reported a computer simulation of a dilute lithium–ammonia solution. The valence electron of a single lithium atom was treated by a quantum path integral Monte Carlo (PIMC) technique, whereas the positive ion-core and solvent molecules were regarded as classical objects. The minimum ernergy configuration was found to be a dipolar atom or contact ion pair; a fact that was ascertained by carrying out a sequence of PIMC calculations with the centre-of-mass (centroid) of the valence electron charge distribution constrained to various separations from the cation [6]. In experiments, lithium is ionised in liquid ammonia [3]. The disagreement with experiment was attributed to the crude pseudopotential used and, possibly, entropic contributions associated with the solvation process.

In the present paper, we have extended the previous calculations on lithium to include two other alkali metals (Na and Cs). In addition to the attractive-core Shaw-type pseudopotential used in [6], we investigate a potential more suitable for heavier alkali metals, where the repulsion between the atom core and the valence electron is more pronounced. As in our earlier works on electron solvation in liquid ammonia [7–9], we employed the staging algorithm [10, 11] to accelerate the convergence of the MC simulation.

This article is arranged as follows. In section 2, we describe the equilibrium correlation functions used to probe the electronic wavefunction and the liquid structure near the positive alkali ion. In section 3, results of the classical simulation of the Li^+, Na^+ and Cs^+ ions in ammonia are given, along with details of the ion-ammonia intermolecular potential. In section 4, the PIMC simulations results for the three alkali *atoms* in ammonia are presented, and the effect of different electron–ion pseudopotentials is discussed. Anticipating our results, we will see that the use of a more refined pseudopotential leads to increasing propensity to ionisation and closer accord with experiment. This article ends with a brief discussion.

2. Equilibrium correlation functions

In the PIMC approach, the electron is represented as an isomorphic ring polymer, or necklace, composed of P segments, or beads, and the solvent molecules by a combination of charge and mass sites. Certain correlation functions involving the valence electron have been monitored during the course of the simulations [7–9].

The electron (centroid)–solvent (site) correlation functions are used to probe the radial distribution of the molecules surrounding the electron. They are defined as

$$g_{\text{cm-}\alpha}(r) = \frac{1}{\rho_\alpha}\left\langle \sum_{n\in\alpha} \delta(\boldsymbol{r} + \boldsymbol{r}_{\text{cm}} - \boldsymbol{r}_n)\right\rangle \tag{1}$$

where ρ_α is the density of α sites, and the brackets denote an average over the MC run. The sum runs over the α sites on each molecule and $\boldsymbol{r}_{\text{cm}}$ is the location of the centroid of the electron polymer. The average orientation of solvent molecules in the vicinity of

the electron cloud is described by the electron (centroid)–solvent (dipole) correlation function

$$P_{cm}(\beta) \propto \left\langle \sum_i \delta(\cos\beta_{cm\text{-}i} - \cos\beta) \right\rangle \tag{2}$$

where

$$\cos\beta_{cm\text{-}i} = (\boldsymbol{R}_i - \boldsymbol{r}_{cm}) \cdot \boldsymbol{d}_i / |\boldsymbol{R}_i - \boldsymbol{r}_{cm}| d_i. \tag{3}$$

Here, $\boldsymbol{R}_i$ and $\boldsymbol{d}_i$ are, respectively, the position vector of the centre of mass and dipole-moment vector of the solvent molecule with the index i. The sum over the index i includes only those molecules in the immediate vicinity of the electron centroid, i.e., those belonging to the first solvation shell.

Two distribution functions directly involve the positive alkali ion. The first is the electron–ion correlation function

$$g_{e\text{-ion}}(r) = \frac{1}{P} \left\langle \sum_{s=1}^{P} \delta(\boldsymbol{r} + \boldsymbol{r}_{ion} - \boldsymbol{r}_s) \right\rangle \tag{4}$$

where $\boldsymbol{r}_s$ is the position of the sth polymer bead and P the total number of beads. The second is the ion–molecule dipole correlation function which characterises the orientation of the solvent molecules around the positive ion. It is defined in a fashion analogous to $P_{cm}(\beta)$, namely

$$P_X(\beta) \propto \left\langle \sum_i \delta(\cos\beta_{X\text{-}i} - \cos\beta) \right\rangle \tag{5}$$

where

$$\cos\beta_{X\text{-}i} = (\boldsymbol{R}_i - \boldsymbol{r}_X) \cdot \boldsymbol{d}_i / |\boldsymbol{R}_i - \boldsymbol{r}_X| d_i \tag{6}$$

with $\boldsymbol{r}_X$ the position of the ion X. Some insights into the nature of the electron state are provided by the imaginary time correlation function, defined as [12]

$$R^2(\tau) = \frac{1}{P} \left\langle \sum_i |\boldsymbol{r}(\tau_i + \tau) - \boldsymbol{r}(\tau_i)|^2 \right\rangle \tag{7}$$

where the sum is extended to all the contributions from the electron at imaginary times differing from each other by multiples of $\tau = \hbar\beta/P$. The value of $R(\tau)$ at half-chain length is related to the electron thermal wavelength by the equation

$$R(\beta\hbar/2) = \sqrt{3}\lambda_T/2. \tag{8}$$

Two aspects of $R(\tau)$ reveal the nature of the electron state: an initial rapid rise with τ followed by a nearly constant region, signals that the electron is in a compact state and that the ground state is dominant, whereas a parabolic dependence implies an extended electron state [13].

3. Li^+, Na^+, and Cs^+ in liquid ammonia

3.1. Intermolecular potentials

To date, most of the theoretical studies on ionic solvation have involved water as the solvent. Alkali ions in water have been studied by molecular dynamics and Monte Carlo

Table 1. Lennard-Jones parameters for alkali ion–ammonia interactions.

	Li^+	Na^+	Cs^+
ε (kJ mol^{-1})	5.5	7.0	14.0
σ (Å)	2.07	2.20	2.90

techniques, and a variety of interaction potentials for these systems are readily available in the literature. Unfortunately, there is almost a complete absence of studies for liquid ammonia. In [14], a simple model potential for the Li^+ ion–ammonia interaction was devised. The same model is used in this article. For Na^+ and Cs^+ solvated in ammonia, our potential parameters are partly derived from SCF calculations at the 6-31G* level [15]. These *ab initio* calculations showed that the intermolecular interaction between ammonia and alkali ions is dominated by electrostatic ion-dipole contributions. In our model, the Coulombic potential arises from an interaction between the unit-positive charge on the cation and four charge sites distributed on the ammonia molecule. The magnitudes and positions of the four ammonia charges were taken from a potential model for liquid ammonia [16].

A Lennard-Jones (12–6) potential between the ammonia nitrogen atom and the cation was used to handle the short-range repulsion and dispersion contributions. As in [14], the parameters of the Lennard-Jones potential have been fitted to the dimer energy and equilibrium distance given by the SCF calculations. In effect, polarisation effects are included at the pair level. Table 1 reports the potential parameters employed for the three cations.

The model potential chosen for ammonia–ammonia interactions is the same as the one described in our previous articles dealing with an excess electron in ammonia [7–9]. In brief, the ammonia intermolecular potential consisted of a nitrogen–nitrogen Lennard-Jones (12–6) interaction, plus interactions between four point charges on each molecule [16].

3.2. Classical MC calculations

3.2.1. Simulation details. Classical MC simulations were performed on a periodically replicated system composed of 250 ammonia molecules and an alkali ion at a molar volume $V = 26.5$ cm^3 mol^{-1} and temperature $T = 260$ K. The ammonia molecules were moved using the standard Metropolis importance sampling algorithm [17], while the alkali ion was kept fixed in the centre of the box. A spherical cut-off at 8.0 Å was employed for all the interactions. In this classical simulation, a MC pass was defined as a sequence of trial moves of randomly chosen ammonia molecules. The length of this sequence equalled the number of molecules in the simulation box. Each move of an ammonia molecule involved translation of the molecular centre-of-mass and rotation of the molecular intertial frame using quaternians [18]. For each type of move, the acceptance rate was maintained around 40%. Typically, the simulations were run for 5000 passes following a period of 2000 passes of equilibration, which allowed the ammonia molecules to adapt to the presence of the ion.

3.2.2. Structure. The basic structure of the solvent ammonia molecules around an ion can be obtained from the two atom–atom correlation functions $g_{XN}(r)$ and $g_{XH}(r)$, where

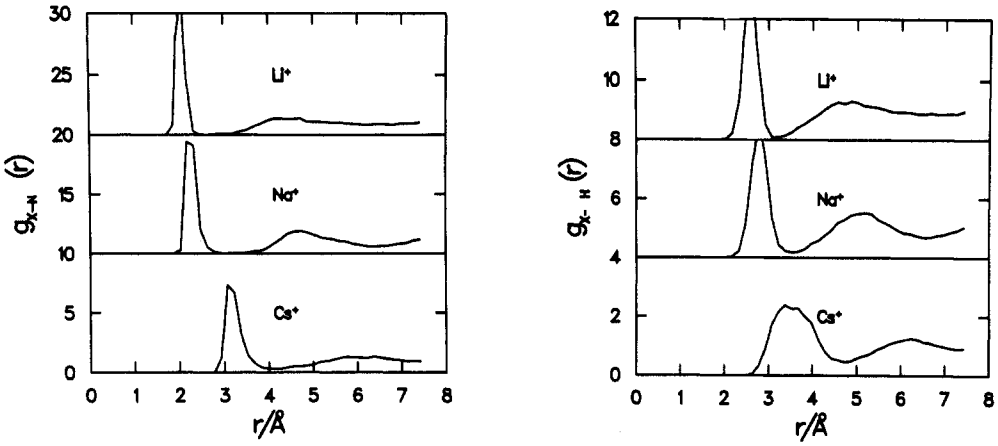

(*a*) (*b*)

Figure 1. Distribution of solvent nitrogen (*a*) and hydrogen (*b*) atoms, with respect to Li^+, Na^+ and Cs^+.

Table 2. Structural data for alkali ions solvated in ammonia.

	r (X–N) (Å)	r (X–H) (Å)	θ (deg)	n_N	n_H
Li^+	2.05	2.62	3	4	12
Na^+	2.25	2.77	1	5	15
Cs^+	3.15	3.37	18	10	35

X = Li^+, Na^+, and Cs^+. Further information on the orientational order around the cation can be gathered from the ion-dipole correlation function defined in section 2.

The functions $g_{XN}(r)$ and $g_{XH}(r)$ for the three ions are plotted in figure 1. The positions at which the first peaks occur are reported in table 2. Except for Cs^+, the separation between the nitrogen and the ions are very close to the value of the parameter σ in the respective Lennard-Jones potentials (see table 1).

The results in figure 1 show that the first peak in $g_{XN}(r)$ is always very strong, primarily due to the very pronounced electrostatic interaction between the ion and the moleules in the first solvent sheath. The height of the peak decreases on going from lithium to caesium. For lithium and sodium, the first minimum in $g_{XN}(r)$ actually falls to zero, and even for caesium it has a very small value. The ammonia molecules of the second solvation shell are less strongly coordinated to the ion and behave like a normal fluid. Sodium yields the sharpest second peak $g_{XN}(r)$.

The average angle β, between the molecular dipole and the vector drawn from the ion to the nitrogen of the first nearest neighbours, can be derived from the positions of the first peaks in both $g_{XN}(r)$ and $g_{XH}(r)$. The results are listed in table 2. Figure 2 shows the calculated distribution of β. The deviation from $\beta = 0$ predicted by *ab initio* calculations on X–NH_3 dimers is very small for the two smallest cations, but more marked for caesium [15]. In solution, more than one orientation contributes to the main peak in $g_{CsH}(r)$, as shown by its sizable width.

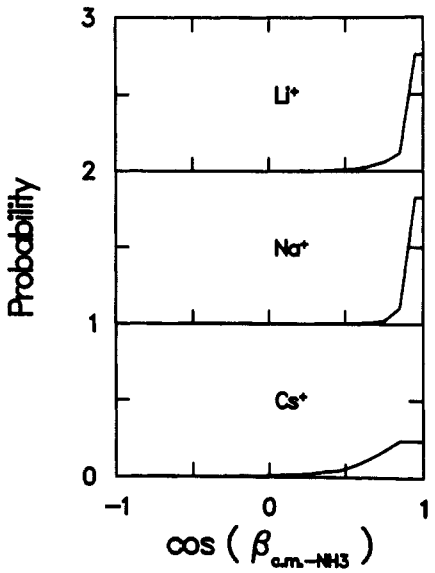

Figure 2. Ion–NH_3 dipole correlation functions for Li^+, Na^+ and Cs^+.

Table 3. Energetics of solvation for a single alkali ion in a system of 250 ammonia molecules. $\langle E_R \rangle$ is the reorganisation energy of the liquid, $\langle E_C \rangle$, $\langle E_D \rangle$ and $\langle E_T \rangle$ are, respectively, the Coulombic, Lennard-Jones and the total energies of the ion, $\langle \Delta E_S \rangle$ is the solvation energy; energies are in kJ mol^{-1}.

	$\langle E_R \rangle$	$\langle E_C \rangle$	$\langle E_D \rangle$	$\langle E_T \rangle$	$\langle \Delta E_S \rangle$
Li^+	1.19	−3.44	0.01	−3.43	−2.24 ± 0.01
Na^+	1.24	−3.29	−0.08	−3.37	−2.13 ± 0.01
Cs^+	1.00	−2.30	−0.61	−2.91	−1.91 ± 0.01

The coordination number, n_N, is usually defined as the mean number of molecules in the cation's first solvation shell, where the separation $r = r_{min}$, at which the function $g_{XN}(r)$ reaches its first minimum, defines the spatial extent of this first shell. For Li^+ and Na^+ r_{min}, and hence the value of n_N, is better defined than for Cs^+. The various coordination numbers for the three cations are listed in table 2. Their values are in agreement with chemical experience and neutron diffraction experiments [19]. In the case of Cs^+, the number of hydrogens in the first shell is not equal to $3 \times n_N$ as for the other cations (see table 2). This indicates that a few H-atoms of ammonia molecules in the second solvation shell are able to penetrate into the first shell.

Results pertaining to the equilibrium energetics for alkali ions solvated in liquid ammonia are given in table 3. It is observed that all three ions have a negative solvation energy and that the major contribution to the energy is supplied by the electrostatic component. Also, on going from the smallest ion to the largest, the contribution from the atom–atom interactions increases noticeably. The solvation of an ion is necessarily acompanied by some change in the structure of the fluid. Table 3 includes the solvent reorganisation energy, relative to the energy of the pure liquid; the latter was obtained from an additional classical MC simulation.

4. Alkali atoms in ammonia

4.1. The pseudopotential problem

In our previous simulation of a lithium atom in liquid ammonia, the ion–electron interaction was handled by using a local pseudopotential taken from solid-state calculations [20]. The potential has the following functional form

$$\begin{aligned} V_{e^-\text{-H}}(r) &= -Q_H e^2/|\boldsymbol{r} - \boldsymbol{R}_H| \qquad |\boldsymbol{r} - \boldsymbol{R}_H| \geqslant R_c \\ V_{e^-\text{-H}}(r) &= -Q_H e^2/R_c \qquad\qquad |\boldsymbol{r} - \boldsymbol{R}_H| < R_c. \end{aligned} \tag{9}$$

The value of the parmeter R_c in (9) for each of the alkali metals can be calculated by fitting to the experimental first ionisation energies, namely, Li, 5.39 eV; Na, 5.14 eV; and Cs, 3.89 eV [20]. A similar model pseudopotential was used by Parrinello and Rahman [21] in their pioneering path-integral simulation of an F centre in molten KCl, in order to handle the interactions between the electron polymer chain and the potassium ion.

The simplicity (only one parameter) of the pseudopotential is essential to its use in a PIMC simulation. Unfortunately, this is also its major limitation. The constant negative potential energy for $r \leqslant R_c$ can produce an unphysically high valence s-electron density inside the ion core. This probelm was not important in early band structure calculations where attractive core pseudopotentials were mostly used. Given the nearly free-electron nature of the Bloch energy bands of most of the non-transition metals, pseudopotential models were chosen to give a rapid damping of the potential for large wave vectors in reciprocal space [20, 22, 23].

Repulsive-core ion-electron pseudopotentials have been used in the past mainly in the study of the structural properties of elemental metals and binary compounds. One such study by Andreoni *et al* [24] proposed a simple pseudopotential that depends on the angular momentum quantum number l. It can be written as

$$V_l(r) = -Ze/r + W_l(r) \tag{10}$$

where Z is the core charge ($Z = 1$ for alkali metals), $W_l(r)$ is a short-range potential

$$W_l(r) = A_l \exp(-\gamma_l r)/r^2. \tag{11}$$

A_l and γ_l are the parameters that describe the interaction of the valence electron with core electrons. $W_l(r)$ contains contributions from short-range orthogonality, electrostatic and exchange interactions. The interaction is positive if some of the core electrons have the same angular momentum as the valence electrons. In this case, $W_l(r)$ is dominated by the repulsive orthogonalisation term. Instead, when the valence electron is in a different angular momentum state, the potential incorporates only the electrostatic and exchange contributions, since the valence and core electrons are already orthogonal. The non-locality of this potential model does not prevent its use in a PIMC simulation. In fact, it may be inferred that the valence electron ground state of an alkali metal in liquid ammonia is mainly an s type state. Therefore, it is not unreasonable to use an ion–electron interaction with only the potential parameters corresponding to $l = 0$. Both attractive core (AC), (9), and repulsive core (RC), (10), potentials have been used in this study. In table 4, we report the parameters for both types of pseudopotential for Li, Na, and Cs.

Table 4. Parameters of the AC and RC electron–ion pseudopotentials. R_c is defined in (9), while A_0 and γ_0 are defined in (11). All parameters are in atomic units.

	R	A_0	γ_0
Li^+	2.885	2233	6
Na^+	3.482	6820	6
Cs^+	4.887	1.309×10^6	6

4.2. Details of the simulations

The atom–ammonia system was studied using the same simulation technique as in our earlier work [6]. In this particular application of the path-integral Monte Carlo method, known as the staging algorithm [10], a necklace of classical pseudo-particles representing the electron is partitioned in a set of P_a primary beads connected by P_b secondary beads. The primary beads, and also the solvent molecules, are moved by the Metropolis importance sampling scheme [17], using weights determined by direct sampling of secondary chain configurations.

The number of beads in the primary chain and each secondary chain configuration were, respectively, $P_a = 128$ and $P_b = 8$. Accordingly, the total electron discretisation was $P = P_a P_b = 1048$. The weight of a link connecting two adjacent beads of the primary chain was evaluated from the contributions of 100 distinct secondary chain configurations. Each MC pass involved the attempted move of all beads in the primary chain, with the corresponding sampling of the secondary chains, and several times (5 to 10), the totality of ammonia molecules. The positive ion was kept fixed at the centre of the simulation box. The PIMC calculations were carried out under the same conditions of temperature, density, and size of the simulation box as in the classical simulations discussed previously ($T = 260$ K, $N = 250$, and $V = 26.5$ cm^3 mol^{-1}).

Before the simulation was initiated, the discretisation of the electron was checked against the reproducibility of the atomic spectroscopic term value. In all cases, the calculated PIMC electron total energy for the isolated atom matched the experimental value within a few per cent.

4.3. Li in liquid ammonia

Our previous PIMC calculation [6] suggested that a Li atom in ammonia is unstable and forms a contact-ion pair in which the valence electron charge is polarised by the surrounding solvent molecules. However, no spontaneous ionisation was observed. The Li atom was subsequently ionised by a series of calculations in which the electon centroid was constrained to increasing distances from the ion. In this way, the activation energy of the ionisation process was estimated. Unfortunately, since this MC simulation did not directly calculate the chemical potential it was not clear if the omitted entropic contribution could stabilise the ionised form with respect to the contact-ion pair.

In the following section, we present new results for lithium in ammonia obtained for the RC potential and compare with those obtained previously with the AC potential [6, 25].

4.3.1. Results. The initialisation of the Li-ammonia system was carried out along the following lines: a compact isomorphic electron polymer ws inserted into an equilibrated

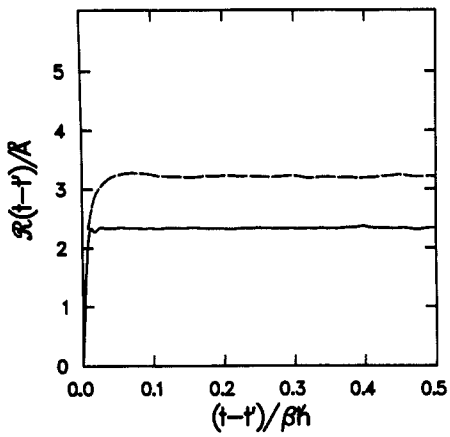

Figure 3. Imaginary time-correlation functions for the Li valence electron, obtained using AC (full curve) and RC (broken curve) pseudopotentials.

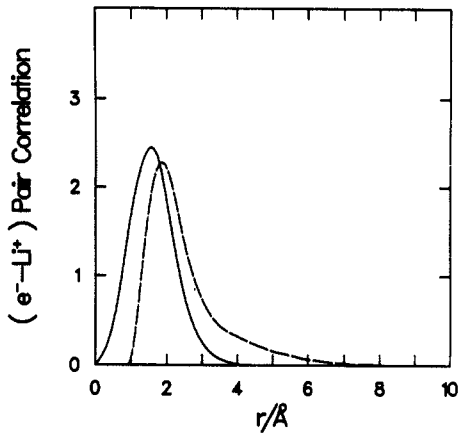

Figure 4. Electron bead–Li^+ correlation functions (in arbitrary units) obtained from the PIMC calculation carried out using AC (full curve) and RC (broken curve) pseudopotentials.

configuration of the liquid plus a cation taken from the classical calculation described in section 3. Initially, the beads of the primary chain were randomly arranged to give a centroid position just outside the ion core region and a correlation length $R(\beta/2) = 2$ Å. The electron was then allowed to adapt to the ion–ammonia potential fields by moving the beads for 100 passes while the coordinates of the solvent molecules were kept unchanged. The simultaneous sampling of the solvent and electron phase space then followed. After 500 passes needed to equilibrate the solvent molecules around the Li atom, 2000 more passes of data acquisition and averaging were required to reach an acceptable stability of the energies.

(i) *Electron wavefunction*. At the end of both the AC and RC simulations, the electron was found in a compact state bound to the Li^+. The imaginary time correlation functions for each case are shown in figure 3. It is clear from this figure that use of the RC pseudopotential yields a more expanded spatial distribution of the electron beads; the electron correlation lengths were found to be 2.34 Å and 3.21 Å for the AC and RC calculations, respectively. The corresponding value for the solvated electron in ammonia is 4.02 Å [25].

Both calculations found the solvated Li atom to be in a dipolar state in which the electron centroid was separated from the ion by a relatively small distance ξ. The RC pseudopotential produced the largest atomic polarisation with $\xi = 1.5$ Å, whereas this separation was $\xi = 0.54$ Å for the AC pseudopotential; the resulting dipole moments in the AC and RC calculations are, respectively, 2.6 D and 7.2 D.

The polarised Li atom obtained in the present simulations has been interpreted in the past due to a dipolar excitonic state [26]. Accordingly, the dipole moment of Li is a hybrid state formed by the superposition of 2s and 2p states. Arguments, based on the continuum dielectric theory, showed that the resulting polarisation induced in the polar fluid is likely to stabilise this state against the energy increase produced by hybridisation [26].

Additional information about the size and, to a lesser extent, the shape of the electron wavefunctions can be obtained from the Li^+-electron pair correlation function shown in

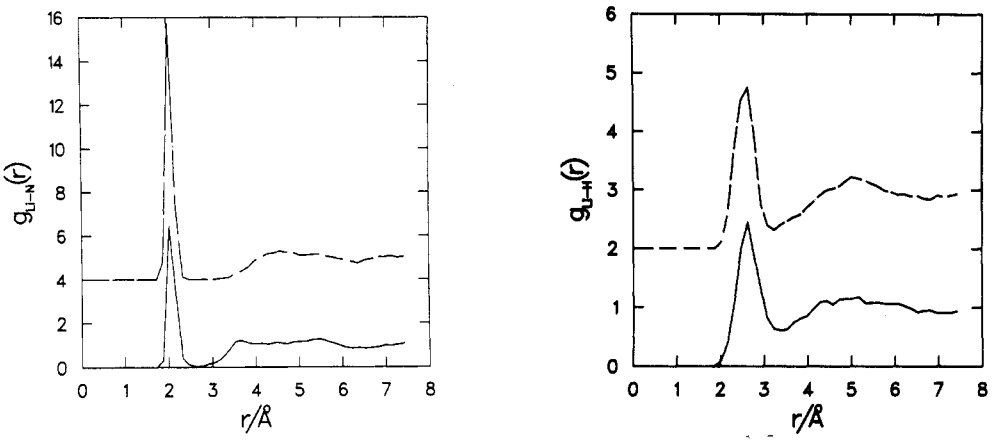

Figure 5. Pair-correlation functions for Li in liquid ammonia, obtained using AC (full curve) and RC (broken curve) pseudopotentials; (*a*) Li–N and (*b*) Li–H.

figure 4. As expected, for the RC potential the inner core becomes a region excluded to the electron. Consequently, there is a much deeper penetration of the eletron cloud into the Li^+ solvation shells. The curves plotted in figure 4 indicate that the change in pseudopotential leads to only a modest shift in the maximum of the electron wavefunction.

(ii) *Liquid structure around the Li atom.* The structure of liquid ammonia in the region surrounding the Li atom (Li^+ plus electron) is best characterised by the Li^+-ammonia and electron centroid-ammonia pair correlation functions. These correlation functions, resulting from the AC and RC calculations, are plotted in figures 5 and 6.

The large polarisation of the Li atom resulting from the use of the RC pseudopotential is the cause of the intense first peak in the $g_{Li^+N}(r)$. The peak height is now comparable to the one calculated from the simulation of the classical ion (recall figure 1), which in turn is associated with strongly coordinated ammonia molecules in the first solvation shell of the ion. The corresponding peak in the AC calculation is much less intense. This can be explained by noticing that the orientation of ammonia molecules in the Li first-solvation shell favoured by the electron is opposite to that desired by the Li^+, and *vice versa*. These competing effects are curtailed when the ion and the electron beads are farther apart. The presence of the electron on the Li^+ therefore induces a decrease in the Li^+ coordination number. The AC and RC calculations yield, respectively, $n_N = 2$ and $n_N = 3$, compared with the value $n_N = 4$ given by the calculation of the classical ion (recall table 2).

The integration of the two functions in figure 5(*b*) yields rather comparable coordination numbers. The RC calculation gives 9 H atoms in the Li^+ first-solvation shell, which is very close to $3 \times n_N$. However, the AC simulation indicates a sizeable interpenetration of the first- and second-solvation shell H-atoms, since there are 11 coordinated H atoms, compared to the expected six. The average of the angle β, defined in section 3.2, calculated with the two pseudopotentials are not significantly different from those of the classical ion.

The functions $g_{cm-N}(r)$ and $g_{cm-H}(r)$ in figure 6 show relatively sharp and intense peaks, which contrast with the results for the solvated electron. The less polarised Li

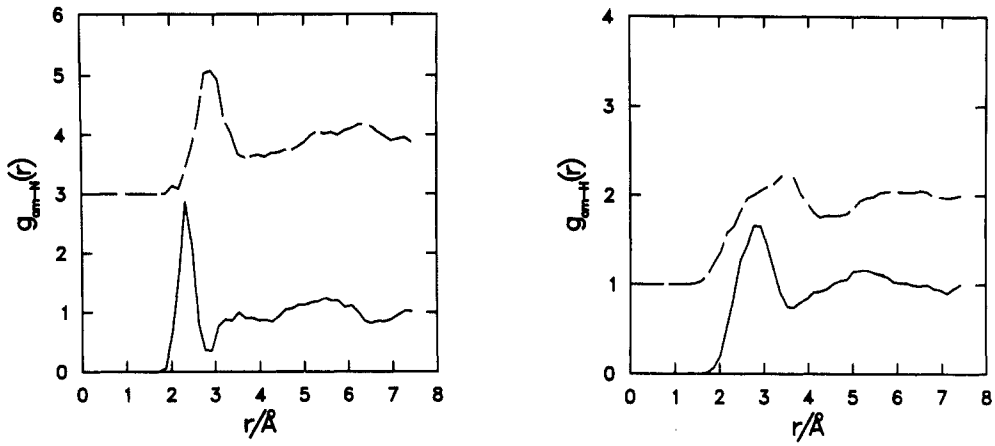

(*a*) (*b*)

Figure 6. Pair-correlation functions for solvent atoms, with respect to the Li valence electron centroid, obtained using AC (full curve) and RC (broken curve) pseudopotentials: (*a*) N and (*b*) H.

atom in the AC simulation yielded a $g_{cm-N}(r)$ which reproduced many of the features of the corresponding correlation function for Li^+ (figures 5(*a*) against 6(*a*)). The same trend was observed for the $g_{cm-H}(r)$ (figures 5(*b*) against 6(*b*)). These findings are related to the rather short distance ξ separating the contact-ion pair and to the small electron-average diameter. As expected, the larger correlation length and increased polarisation of the Li atom produced by the RC pseudopotential dereased the structural characteristics of the relative (cm–N) and (cm–H) correlation functions. This is particularly visible in $g_{cm-H}(r)$. The coordination numbers found for the electron and Li^+ in the AC simulation were identical; two ammonia molecules on average were coordinated to the electron. In the RC calculation, instead, the electron coordination number was about 4, compared to 3 for Li^+.

Further information on the orientational ordering of the ammonia molecules coordinated to the contact-ion pair can be derived from the respective dipole correlation functions plotted in figure 7. Only the contributions from solvent molecules within 4 Å from the Li^+ or electron centroid were included in the computation of these correlation functions. In both calculations, the ammonia molecules around the electron are seen to be influenced by the nearby Li^+, this being the main cause of the peaks at $\cos\beta = 0.7$ and 0.9, respectively, in figures 7(*a*) and 7(*b*). The tail of the distribution centred around $\cos\beta = -0.5$ is due to a fraction of solvent molecules bond-oriented towards the electron. The dipole correlation functions for Li^+ (figure 7(*b*)) exhibit intense peaks near $\cos\beta = 1$, corresponding to the fully dipole-ordered case, i.e. $\beta = 0$. The curve obtained from the AC calculation exhibits a weak peak for negative values $\cos\beta$. Pictorial representation of the contact-ion pair formed upon immersion of the Li atom into liquid ammonia is given in figure 8. Based on the RC pseudopotential, the electron is more diffuse than in the case of the AC pseudopotential (see, for example, figure 1 in [6]).

4.4. Cs and Na in liquid ammonia

The PIMC simulations described in the previous section did not lead to a spontaneous

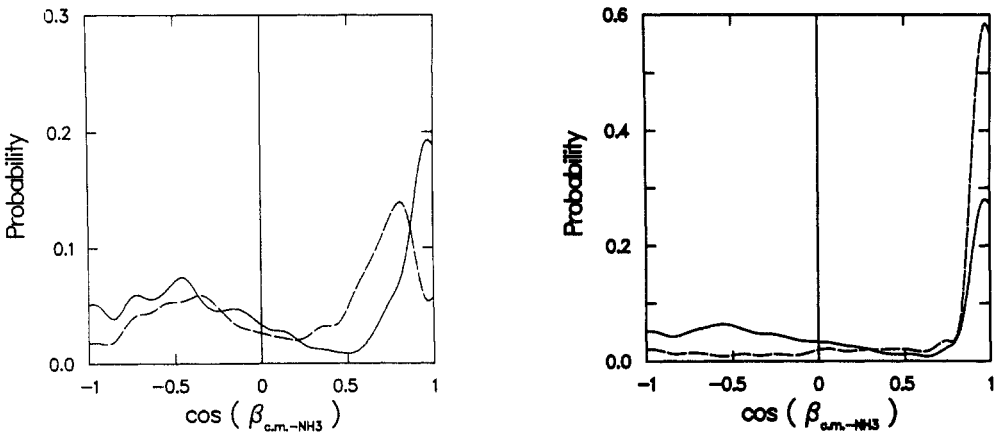

Figure 7. (*a*) Electron and (*b*) Li^+–ammonia dipole correlation functions obtained using the AC (full curves) and RC (broken curves) pseudopotentials.

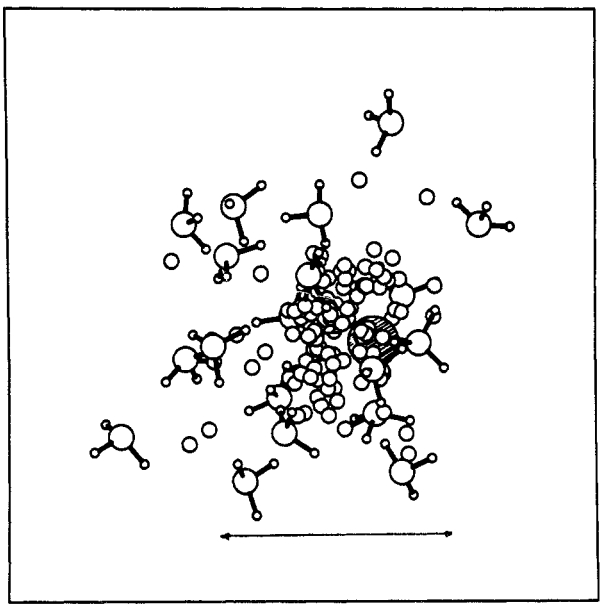

Figure 8. Instantaneous configuration for the contact ion pair (Li^+–e^-) from the RC pseudopotential simulation. The Li^+ ion is shaded. For graphic reasons, only one out of every two primary chain beads is plotted, and the marker indicates 10 Å.

ionisation of a Li atom in liquid ammonia. Although there is no direct experimental evidence to support the presence of contact-ion pairs in solution, it should be noted that neutral Li may be stabilised at low temperature in *solid* ammonia [27]. Hence, the question of possible matastability arises. There is thus a need to evaluate the relative

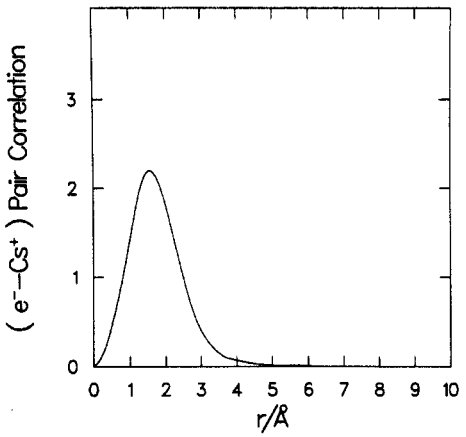

Figure 9. The correlation function of the electron polymer (in arbitrary units) with respect to the Cs^+ ion, calculated using the AC pseudopotential.

free energy of the contact ion-pair with respect to the ionised and solvated Li^+ and e^-. The experimental situation for Na and heavier alkali metals clearly indicate that they are also ionised in liquid ammonia. The main objective of the remaining part of the present PIMC study is to investigate whether or not spontaneous ionisation of Na and Cs is observed in the simulations, unlike the situation for Li.

The physical conditions, the simulation parameters, and the initalisation procedures used in the following PIMC calculations on Cs and Na were identical to those previously specified for the Li calculations in section 3.2.

4.4.1. The dipolar Cs atom. In the case of Li, the AC pseudopotential does not exclude the excess electron from penetrating inside the ion core (recall figure 4). This effect is expected to be even more marked for a a larger ion, where the increased ionic radius prevents the ammonia molecules of the first solvation shell from getting close to the excess electron. In order to verify this supposition, a simulation of the Cs atom in ammonia was performed using the AC potential in table 4. The simulation was initiated following the procedure described in section 4.3.1.

As in the case of Li, the AC pseudopotential readily promoted the formation of a contact ion-pair, Cs^+–e^-. The electron necklace localised at about 0.8 Å from the ion; a situation that produces a Cs dipole moment of approximately 3.9 D. The localised nature of the electron state is also evident from a plot of $R(t - t')$; the average correlation length, $R(\hbar\beta/2) = 2.6$ Å, is very close to that given by the AC pseudopotential for Li. Thus, the electron necklace is now entirely confined to the Cs^+ core region, with only a limited penetration into the first solvent sheath: a fact demonstrated by the drop to near zero at 3.5 Å of the electron–Cs^+ correlation function shown in figure 9.

The Cs^+–N and Cs^+–H pair-correlation functions are plotted in figure 10. There is a decrease in peak height of Cs^+–N with respect to the result for the classical ion shown in figure 1, due to electron screening. The $g_{Cs^+H}(r)$ reveals a splitting in the first peak, produced by two inequivalent hydrogen atoms of the first solvent sheath. This splitting is not resolved in figure 1. The results for the electron centroid–N and –H correlation functions are virtually identical to those obtained for Cs^+–N and Cs^+–H and are, therefore, not shown. The two peaks imply that the NH bond makes angles 39° and 37°, with respect to the Cs^+–N direction. This splitting is responsible for the broad peak around $\cos\beta \simeq 0.7$ in the Cs–ammonia dipole correlation function plotted in figure 11.

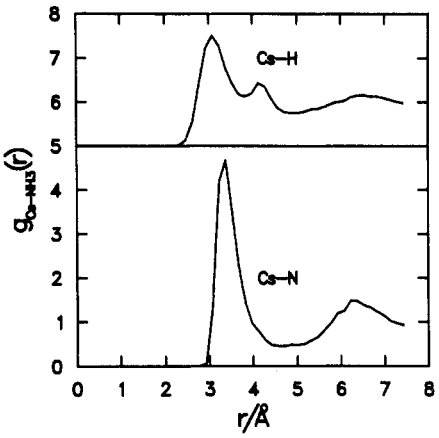

Figure 10. Distribution functions for the solvent nitrogen and hydrogen atoms with respect to the Cs^+ ion, using the AC pseudopotential. The electron centroid–nitrogen and –hydrogen functions (not shown) are virtually identical to those for Cs^+.

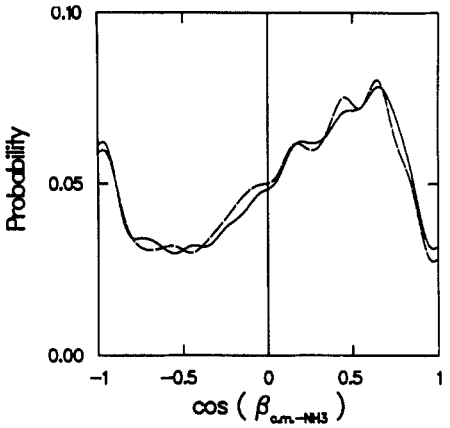

Figure 11. Cs^+– and e^-–ammonia dipole correlation functions from the simulation for the AC pseudopotential. The bold curve is for Cs^+ and the dashed for the electron centroid.

The cut-off for this function was set to 5 Å. The maximum for negative values of cos β is due to those ammonia molecules coordinated to the electron. The dipole-correlation function relative to the centroid of the electron plotted in figure 11 is virtually identical to the Cs^+ dipole function. The coordination number of Cs is 10, unchanged from the results of the classical ion (see table 2).

The conclusion from these results is that the AC pseudopotential produces an unphysical localisation of the electron necklace in the Cs^+ core. We, therefore, next consider a more realistic pseudopotential with a repulsive core.

4.4.2. Ionisation of Cs and Na. Since the contribution from the repulsive core of the pseudopotential is very marked in Na and Cs, the initialisation of the respective simulations was carried out in a cautious manner. First, all of the beads of the electron necklace were inserted in the region outside the minimum in the electron-ion pseudopotential. The solvent molecules were then allowed to adjust to the electron necklace for 200 passes. Next, the polymer beads were sampled for 200 passes, keeping the solvent molecules fixed. Finally, both electron and ammonia molecules were moved.

For both Cs and Na, use of the RC pseudopotential caused the electron to expand into the solvent and to eventually drift away from the ion. This ionisation process occurred spontaneously following the formation (after about 1000 passes) of an extended electron state, peaked at correlation lengths of 15 Å and 12 Å, respectively, for Na and Cs. After 3000 more passes for Cs and 4000 more for Na, the ionisation process culminated in the creation of a solvated cation and a localised-compact solvated electron. This mechanism of ionisation involving a transient quasi-free electron state is in agreement with previously reported results [6] regarding the induced ionisation of Li in ammonia. An example of this intermediate stage—an instantaneous configuration taken from the Na calculation after 2000 passes—is plotted in figure 12.

Examples of electron–Cs^+ correlation functions, calculated at different stages of

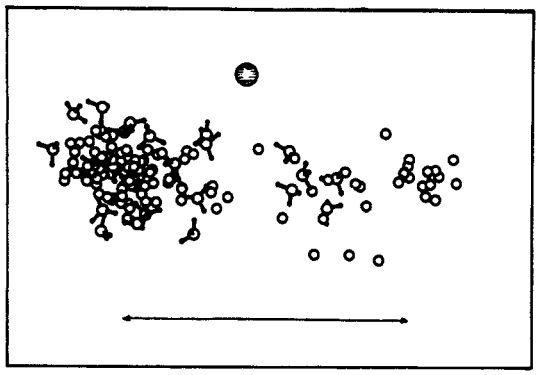

Figure 12. Instantaneous configuration for the pair (Na^+–e^-) from the simulation with the RC pseudopotential. The Na^+ in is shaded. Only the primary chain beads of the electron necklace are plotted. The marker indicates 20 Å.

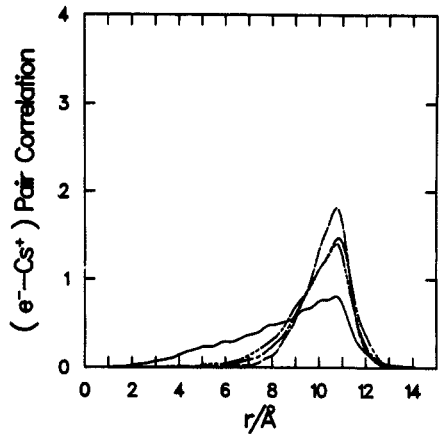

Figure 13. Electron–Cs^+ correlation functions (in arbitrary units) at different stages of the simulation carried out using the repulsive core pseudopotential. The bold curve refers to the situation after 1300 passes, and the dashed curve to 3000 passes.

simulation, are presented in figure 13. These functions clearly indicate the localisation of the electron density at about 11 Å away from the Cs^+. Similar results were obtained for Na; in this case the electron localised at about 14 Å from that Na^+.

5. Discussion

This paper has been concerned with solvation of alkali ions and atoms in liquid ammonia. We have used classical MC simulation to study the structure of an ammonia solvent around Li^+, Na^+ and Cs^+. The simple ion–ammonia intermolecular potentials we employ are able to predict negative solvation energies, and also to reproduce the limited experimental information on coordination numbers for the ions [19].

By using path-integral MC simulation, we have shown that the commonly used [21] AC pseudopotential model [20] leads to the formation of an unphysical dipolar atom when tested, for the case of Cs in ammonia. In contrast, the RC pseudopotential model [24] is able to yield the spontaneous ionisation of Cs and Na in liquid ammonia. Our calculations, therfore, indicate that the minimum energy state for Cs and Na is indeed the fully ionised and separately solvated species; an observation in agreement with experimental evidence.

Although the repulsive core model did not predict spontaneous ionisation of Li in liquid ammonia, it did yield a dipolar Li atom that is much more polarised than in our earlier calculations with the attractive core model. In the absence of a free-energy calculation, ionisation cannot be ruled out as the minimum energy state.

We have shown that the basic behaviour of simple alkali metals in liquid ammonia at infinite dilution can be rationalised in terms of simple potential models for the interacting species. Future work on metal–ammonia solutions will need to move into the regime of more concentrated solutions, i.e., more than one electron. For the alkali metal–molten salt system, calculations have already been reported for several excess

(solvated) electrons [28]. A similar approach could perhaps be employed for the present problem. Other solvents, such as methylamine, should also be considered [29], and the effect of solvent (many-body) polarisation also needs to be investigated rather carefully [30]. Finally, it will be instructive to explore related phenomena in gas-phase clusters—systems eminently suitable to study using molecular-beam techniques [31].

Acknowledgments

M M thanks NSERC for financial support during his graduate studies. The research outlined herein was supported, in part, by the US National Science Foundation under CHE 87 22481 and DMR 88 19885. Some of the calculations were carried out at the JvNC computer centre. We thank Volker Heine for useful suggestions.

References

[1] Thompson J C 1973 *Electrons in Fluids* ed J Jortner and N R Kestner (Berlin: Springer)
[2] Mott N F 1974 *Metal–Insulator Transitions* (London: Taylor and Francis)
[3] Schindewolf U 1984 *Physics and Chemistry of Electrons and Ions in Condensed Matter* ed J V Acrivos, N F Mott and A D Joffe (Dordrecht: Reidel)
[4] Ashcroft N W and Russakoff G 1970 *Phys. Rev.* A **1** 39
[5] Schroeder R L and Thompson J C 1968 *Bull. Am. Phys. Soc.* **13** 397
[6] Sprik M, Impey R W and Klein M L 1986 *Phys. Rev. Lett.* **56** 2326
[7] Sprik M, Impey R W and Klein M L 1985 *J. Chem. Phys.* **83** 5802
[8] Sprik M and Klein M L 1988 *Computer Phys. Rep.* 7 147
[9] Marchi M, Sprik M and Klein M L 1988 *J. Phys. Chem.* **92** 3625
[10] Sprik M, Klein M L and Chandler D 1985 *Phys. Rev.* B **31** 4234
[11] Sprik M, Klein M L and Chandler D 1985 *J. Chem. Phys.* **83** 3042
[12] Chandler D, Singh Y and Richardson D M 1984 *J. Chem. Phys.* **81** 1975
Nichols A L III, Chandler D, Singh V and Richardson D M 1984 *J. Chem. Phys.* **81** 5109
Nichols A L III and Chandler D 1986 *J. Chem. Phys.* **84** 398
[13] Chandler D 1990 Theory of quantum processes in liquids *Liquids, Freezing and the Glass Transition* ed D Levesque, J-P Hansen and J Zinn-Justin (Amsterdam: Elsevier)
[14] Impey R W, Sprik M and Klein M L 1987 *J. Am. Chem. Soc.* **109** 5900
[15] Smith S F, Chandrasekha J and Jorgensen W L 1982 *J. Phys. Chem.* **86** 3308
[16] Impey R W and Klein M L 1984 *Chem. Phys. Lett.* **104** 579
[17] Metropolis N, Rosenbluth A W, Rosenbluth M N, Teller A H and Teller E 1953 *J. Chem. Phys.* **21** 1087
[18] Allen M P and Tildesley D J 1987 *Computer Simulation of Liquids* (Oxford: Clarendon)
[19] Stacy A M and Sienko M J 1982 *Inorg. Chem.* **21** 2294
Chieux P and Bertagnolli H 1984 *J. Phys. Chem.* **88** 3726
[20] Shaw R W 1968 *Phys. Rev.* **174** 769
[21] Parrinello M and Rahman A 1984 *J. Chem. Phys.* **80** 860
[22] Phillips J C and Kleinman L 1959 *Phys. Rev.* **116** 287
[23] Heine V and Abarenkov I V 1964 *Phil. Mag.* **9** 451
[24] Andreoni W, Baldereschi A, Biémont E and Phillips J C 1979 *Phys. Rev.* B **20** 4814
[25] Sprik M, Impey R W and Klein M L 1987 unpublished
[26] Logan D E 1986 *Phys. Rev. Lett.* **57** 782
[27] Meier P F, Hauge R H and Margrave J L 1978 *J. Am. Chem. Soc.* **100** 2108
[28] Selloni A, Car R, Parrinello M and Carnevali P 1987 *J. Phys. Chem.* **91** 4947
[29] Edwards P P 1988 *Nature* **331** 964
Edwards P P, Ellaboudy A, Holton D M and Pyper N C 1988 *Ann. Rep. NMR Spectroscopy* **20** 315
[30] Sprik M and Klein M L 1988 *J. Chem. Phys.* **89** 7556
[31] Honea E C, Homer M L, Labastie P and Whetton R L 1989 *Phys. Rev. Lett.* **63** 394